

Main-group and transition-metal complexes of 1-thia-4,7-diazacyclononane, [9]aneN₂S. Crystal structures of [VOCl₂([9]aneN₂S)]·MeCN, [Fe([9]aneN₂S)₂][ClO₄]₂, [Zn([9]aneN₂S)₂][PF₆]₂, [Ru(cym)([9]aneN₂S)][BPh₄]Cl₂·MeCN (cym = *p*-cymene), [RhCl₃([9]aneN₂S)]·H₂O and [Tl([9]aneN₂S)][ClO₄]

Ulrich Heinzl, Andreas Henke and Rainer Mattes*

Anorganisch-Chemisches Institut der Westfälischen Wilhelms-Universität,
Wilhelm-Klemm-Strasse 8, 48149 Münster, Germany

A series of half-sandwich and sandwich complexes of the nine-membered mixed donor macrocyclic 1-thia-4,7-diazacyclononane ([9]aneN₂S) with metals in different oxidation states has been synthesized and characterized. In each case, the ligand provides tridentate face-capping co-ordination to the metal ion. X-Ray crystallographic structure determinations have been performed for most complexes; [Fe([9]aneN₂S)₂]²⁺ and [Zn([9]aneN₂S)₂]²⁺ display *trans*-octahedral N₄S₂ co-ordination. The metal–nitrogen and metal–sulfur bond distances are greater than the respective lengths in the homoleptic complexes [M([9]aneN₃)₂]²⁺ and [M([9]aneS₃)₂]²⁺ (M = Fe or Zn, [9]aneN₃ = 1,4,7-triazacyclononane, [9]aneS₃ = 1,4,7-trithiacyclononane). In the complexes of metal ions with larger radii, *e.g.* Rh^{III} and Tl^I, the metal–sulfur distances are equal to or smaller than those in the complexes of [9]aneS₃. The difference between the metal–nitrogen and the metal–sulfur bond lengths varies from 0.21 Å to 0.40 Å in the complexes studied. Both λλλ and λδλ conformations of the three chelate rings formed were observed.

The chemistry of 1,4,7-triazacyclononane ([9]aneN₃) and 1,4,7-trithiacyclononane ([9]aneS₃) has been extensively developed over the last decade.¹ Far less is known about the co-ordination compounds of the mixed N,S-donor nine-membered macrocycles 1-thia-4,7-diazacyclononane ([9]aneN₂S)^{2–4} and 1,4-dithia-7-azacyclononane ([9]aneNS₂),⁵ mainly due to the difficulties encountered during their synthesis. The four macrocycles mentioned ideally co-ordinate to triangular faces of tetrahedra, octahedra or trigonal prisms.

The macrocycle [9]aneN₂S features different binding sites in close proximity and has the potential to co-ordinate to both harder and softer ions or molecules. The loss of three-fold symmetry introduces interesting stereochemical consequences. No half-sandwich complexes of [9]aneN₂S have been reported so far, in contrast to [9]aneN₃ and [9]aneS₃. In a more extended study we are presently exploring the co-ordination chemistry of mixed N,S-macrocycles with various ring sizes.⁶ In this paper we report the synthesis and characterization of several half-sandwich and sandwich complexes of [9]aneN₂S with metals in different oxidation states.

Results and Discussion

[VOCl₂([9]aneN₂S)]·MeCN

The reaction of VCl₃ with 1 mol equivalent of [9]aneN₂S in MeCN affords the vanadium(IV) compound [VOCl₂([9]aneN₂S)]·MeCN. Vanadium(III) is oxidized to vanadium(IV) by traces of oxygen during the slow crystallization process. The presence of the VO group and the ligand was confirmed by IR and UV/VIS spectroscopy. The IR spectrum shows sharp ν(NH) absorptions at 3240 and 3200 cm⁻¹, and ν(VO) at 985 cm⁻¹. In the UV/VIS spectrum all three expected vanadyl(IV) d–d transitions are observed, giving a value for *Dq* of 19 800 cm⁻¹. The value is slightly larger than usually found in oxovanadium(IV) complexes with N-, O- or S-donor ligands. The high ligand field exerted

by [9]aneN₂S is confirmed by the EPR parameters at ambient and low temperatures. The ⁵¹V hyperfine coupling constants of *A*_{iso} = 91.2 × 10⁻⁴ cm⁻¹ at *g* = 1.986 and of *A*_{||} = 161.1 × 10⁻⁴ cm⁻¹ at *g*_{||} = 1.965 were established. (The signals of the inner octet, displaying *A*_⊥ and *g*_⊥, were poorly resolved, so these parameters could not be determined.)

Vanadium is octahedrally co-ordinated in [VOCl₂([9]aneN₂S)]·MeCN according to the structure determination. A view of the molecule is shown in Fig. 1. Selected bond lengths and angles are given in Table 1. The sulfur atom of [9]aneN₂S and the terminal oxygen atom are co-ordinated in mutual *trans* positions. The V–O bond is short at 1.632(2) Å and has a strong *trans* influence upon the V–S bond. Its length is 2.689(1) Å. A shorter bond length of 2.634 Å has been observed in [VOCl₂([9]aneS₃)].⁷ Corresponding to the weak bonding of the sulfur atom the VO vibration frequency is shifted to rather high wavenumbers at 985 cm⁻¹. Sulfur co-ordination at the site with the largest metal-to-metal ligand distance is favoured also by the asymmetric structure of [9]aneN₂S. The nitrogen atoms of [9]aneN₂S are strongly co-ordinated in the equatorial plane. The V–N bond lengths of 2.153(2) and 2.150(2) Å are similar to those reported for oxovanadium(IV) complexes of [9]aneN₃,⁸ whereas the V–Cl bond lengths of 2.346(1) and 2.337(1) Å are slightly larger than in the closely related compound [VOCl₂([9]aneS₃)].⁷ The vanadium atom is situated 0.32 Å above the mean plane containing the equatorial ligands Cl(1), Cl(2), N(1) and N(2). The molecules are interconnected in the solid state by weak O···N hydrogen bonds.

[Mn([9]aneN₂S)₂][ClO₄]₂

This compound has been prepared very recently in an independent study,⁹ and the crystal structure has also been reported. The metal ion of the complex cation is situated on a site of 2/*m* symmetry with Mn–N and Mn–S bond lengths of 2.242(7) and 2.625(3) Å, respectively. All ligand atoms show

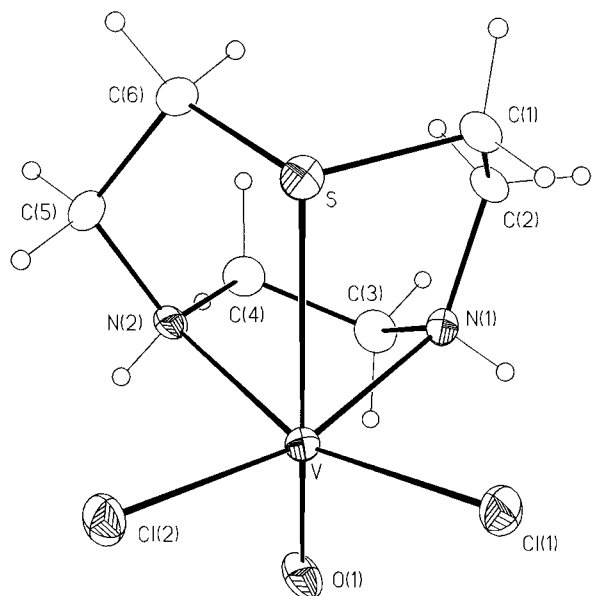


Fig. 1 Structure of $[\text{VOCl}_2([\text{9]aneN}_2\text{S})]$

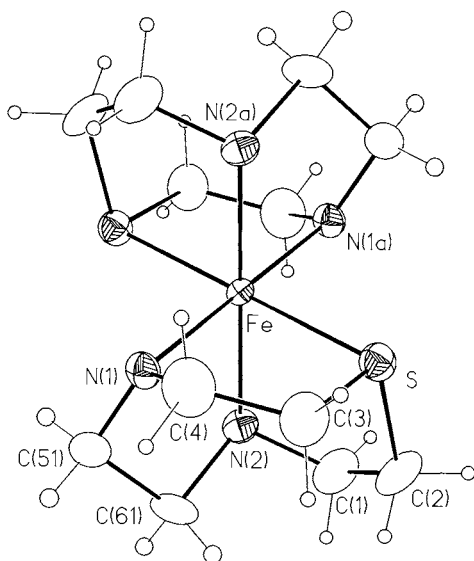


Fig. 2 Structure of the $[\text{Fe}([\text{9]aneN}_2\text{S})_2]^{2+}$ ion

rather high thermal parameters due to disorder. There is no doubt that the compound prepared by us is identical with the complex described.

$[\text{Fe}([\text{9]aneN}_2\text{S})_2][\text{ClO}_4]_2$

The green iron(II) complex was obtained in high yield under an inert atmosphere. The analogous $[\text{Fe}([\text{9]aneN}_2\text{S})_2]\text{Br}_2$ was also prepared. From an ethanolic solution of this compound the dark brown iron(III) complex $[\text{Fe}([\text{9]aneN}_2\text{S})\text{Br}]\text{Br}_2$ could be synthesized by slow crystallization in an open vessel. Its structure is not known, but the iron(III) ion is probably tetrahedrally co-ordinated by Br and the ligand $[\text{9]aneN}_2\text{S}$. The complex $[\text{Fe}([\text{9]aneN}_2\text{S})_2][\text{ClO}_4]_2$ consists of $[\text{Fe}([\text{9]aneN}_2\text{S})_2]^{2+}$ cations situated on crystallographic inversion centres. The cation is depicted in Fig. 2. Selected bond lengths and angles are given in Table 2. The metal centre is *trans*- N_4S_2 co-ordinated. The isolation of both *cis* and *trans* geometric isomers has been achieved so far only for cobalt(III).⁴ The Fe–N(1) and Fe–S bond lengths are 2.072(6) and 2.337(2) Å, respectively. Both values are greater than the respective bond distances in the homoleptic complexes $[\text{Fe}([\text{9]aneN}_3)_2]^{2+}$ and $[\text{Fe}([\text{9]aneS}_3)_2]^{2+}$ where the following bond distances have been found: Fe–N 2.02(1) and Fe–S 2.250(1) Å.^{3,10} Obviously the capability of $[\text{9]aneN}_2\text{S}$ to form

Table 1 Selected bond lengths (Å) and angles (°) for $[\text{VOCl}_2([\text{9]aneN}_2\text{S})]\cdot\text{MeCN}$

V–O	1.632(2)	V–S	2.689(1)
V–N(1)	2.153(2)	V–Cl(1)	2.337(1)
V–N(2)	2.150(2)	V–Cl(2)	2.346(1)
Cl(1)–V–Cl(2)	95.1(1)	O–V–N(1)	95.2(1)
N(1)–V–S	78.6(1)	O–V–N(2)	95.9(1)
Cl(1)–V–N(2)	159.8(1)	O–V–Cl(1)	101.2(1)
N(1)–V–N(2)	78.5(1)	O–V–Cl(2)	99.7(1)
N(2)–V–S	77.6(1)	O–V–S	171.7(1)
Cl(2)–V–N(1)	163.4(1)		

Table 2 Selected bond lengths (Å) and angles (°) for $[\text{Fe}([\text{9]aneN}_2\text{S})_2][\text{ClO}_4]_2$ and $[\text{RhCl}_3([\text{9]aneN}_2\text{S})]\cdot\text{H}_2\text{O}$

$[\text{Fe}([\text{9]aneN}_2\text{S})_2][\text{ClO}_4]_2$			
Fe–S	2.337(2)	Fe–N(2)	2.063(7)
Fe–N(1)	2.072(7)		
S–Fe–N(1)	84.9(2)	S–Fe–N(1a)	95.1(2)
S–Fe–N(2)	84.6(2)	S–Fe–N(2a)	95.4(2)
N(1)–Fe–N(2)	82.5(3)	N(1)–Fe–N(2a)	97.5(3)
$[\text{RhCl}_3([\text{9]aneN}_2\text{S})]\cdot\text{H}_2\text{O}$			
Rh–S	2.246(1)	Rh–Cl(1)	2.396(1)
Rh–N(1)	2.036(3)	Rh–Cl(2)	2.368(1)
Rh–N(2)	2.040(3)	Rh–Cl(3)	2.358(1)
S–Rh–Cl(1)	177.8(1)	Cl(1)–Rh–Cl(3)	91.3(1)
S–Rh–Cl(2)	89.6(1)	Cl(2)–Rh–Cl(3)	92.8(1)
Cl(1)–Rh–Cl(2)	91.3(1)	S–Rh–N(1)	87.2(1)
S–Rh–Cl(3)	90.7(1)	Cl(1)–Rh–N(1)	90.7(1)
Cl(2)–Rh–N(1)	93.0(1)	Cl(3)–Rh–N(1)	173.8(1)
S–Rh–N(2)	87.6(1)	Cl(1)–Rh–N(2)	91.4(1)
Cl(2)–Rh–N(2)	175.4(1)	Cl(3)–Rh–N(2)	90.9(1)
N(1)–Rh–N(2)	83.2(1)		

strong bonds to iron(II) is lower than that of both related, more symmetrical ligands. Iron(II) is in the low-spin state in the complexes of all three nine-membered macrocycles.

The apparent symmetry of the cation $[\text{Fe}([\text{9]aneN}_2\text{S})_2]^{2+}$ in the crystal lattice is close to $2/m$. This symmetry is incompatible with any of the possible configurations of the three chelate rings. A close inspection of the vibrational ellipsoids showed, however, that the carbon atoms in the N–C–C–N moiety are disordered. The disorder could be resolved by introducing split positions and is caused by the presence of λ - and δ -configured *N,N*-chelate rings at a single crystal site. Of the two remaining *N,S*-chelate rings one displays a δ configuration, the other λ . An independent determination of the structure of $[\text{Fe}([\text{9]aneN}_2\text{S})_2][\text{ClO}_4]_2$ has been reported recently.*

$[\text{Zn}([\text{9]aneN}_2\text{S})_2][\text{PF}_6]_2$

The reaction of $\text{Zn}(\text{acac})_2$ (*acac* = acetylacetonate) with $[\text{9]aneN}_2\text{S}$ in the ratio 1:2 yields the bis-complex $[\text{Zn}([\text{9]aneN}_2\text{S})_2]^{2+}$, which could be crystallized as its PF_6^- salt. Experiments failed to prepare the mono-complex $[\text{ZnCl}([\text{9]aneN}_2\text{S})]^+$, with four-fold co-ordination of the metal, by reaction of ZnCl_2 with $[\text{9]aneN}_2\text{S}$ in the ratio 2:1. Instead the compound $[\text{Zn}([\text{9]aneN}_2\text{S})_2][\text{ZnCl}_4]$ was obtained in high yield. The structures of both the PF_6^- and the $[\text{ZnCl}_4]^{2-}$ salts have been determined. Fig. 3 shows the cations and Table 3 contains selected bond

* The observed symmetry of $[\text{Fe}([\text{9]aneN}_2\text{S})_2][\text{ClO}_4]_2$ is clearly monoclinic; $[\text{Fe}([\text{9]aneN}_2\text{S})_2][\text{ClO}_4]_2$ and $[\text{Mn}([\text{9]aneN}_2\text{S})_2][\text{ClO}_4]_2$ are isostructural. The assignment of orthorhombic symmetry to the structure of $[\text{Mn}([\text{9]aneN}_2\text{S})_2][\text{ClO}_4]_2$ ⁹ is the reason that the structure seems to be extensively disordered in the anionic and cationic moieties, and that the disorder could not be resolved.

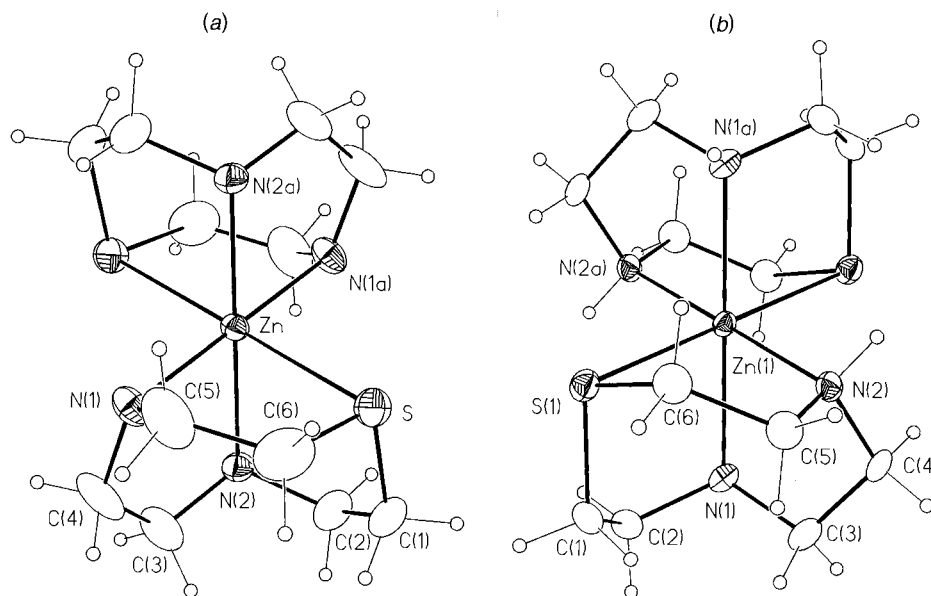


Fig. 3 Structure of $[\text{Zn}(\text{[9]aneN}_2\text{S})_2]^{2+}$ in the $[\text{PF}_6]^-$ salt (a) and the $[\text{ZnCl}_4]^{2-}$ salt (b)

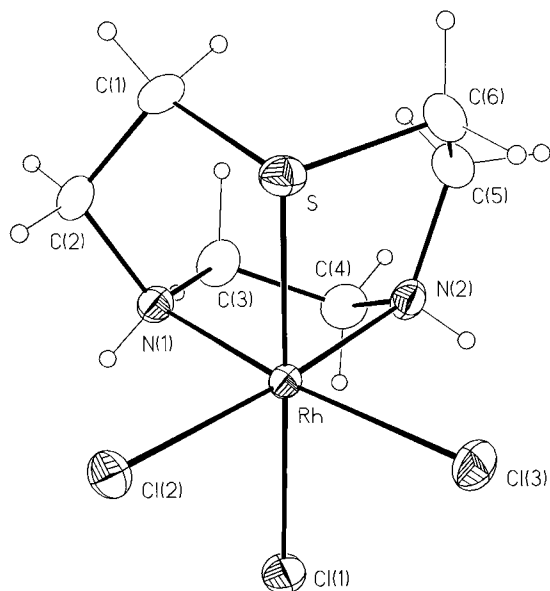


Fig. 4 Structure of $[\text{RhCl}_3(\text{[9]aneN}_2\text{S})]$

lengths and angles of both compounds. The Zn–S bond lengths of 2.548(2), 2.550(3) and 2.555(3) Å are very similar in these compounds, but the Zn–N bond lengths seem to be slightly different in the PF_6^- and the ZnCl_4^{2-} salts. The mean values are 2.144 and 2.170 Å, respectively. The effect is probably caused by strong hydrogen bonds between the N–H and Zn–Cl bonds, which connect anions and cations to a three-dimensional net. In the complexes of fourteen-membered azamacrocycles the Zn–N distances vary from 2.03 to 2.19 Å with a mean value of 2.11 Å.¹¹ The bond lengths in the present complexes are close to the upper limit of the specified range. In the $[\text{Zn}(\text{[9]aneS}_3)_2]^{2+}$ ion the mean Zn–S bond length is 2.494 Å.¹² As in the case of the iron(II) complexes the bond length in the mixed-donor complex is greater than respective bond distance in the homoleptic complex. The structure of the $[\text{Zn}(\text{[9]aneN}_3)_2]^{2+}$ ion is so far unknown.

In the PF_6^- salt the carbon atoms within the N–C–C–N moiety are disordered. This situation has been discussed above for $[\text{Fe}(\text{[9]aneN}_2\text{S})_2][\text{ClO}_4]_2$. The unit cell contains $\lambda\lambda\delta$ and $\delta\lambda\delta$ configurational isomers at a single site. In the ZnCl_4^{2-} salt the two crystallographically independent complex ions clearly display symmetrical $\lambda\lambda\lambda$ or $\delta\delta\delta$ configuration of the chelate rings.

Table 3 Selected bond lengths (Å) and angles (°) for $[\text{Zn}(\text{[9]aneN}_2\text{S})_2][\text{PF}_6]_2$ and $[\text{Zn}(\text{[9]aneN}_2\text{S})_2][\text{ZnCl}_4]$

	$[\text{Zn}(\text{[9]aneN}_2\text{S})_2][\text{PF}_6]_2$	$[\text{Zn}(\text{[9]aneN}_2\text{S})_2][\text{ZnCl}_4]$	
Zn–S(1)	2.548(2)	2.550(3)	2.555(3)
Zn–N(1)	2.160(5)	2.206(6)	2.159(8)
Zn–N(2)	2.149(5)	2.162(6)	2.153(7)
S(1)–Zn–N(1)	82.7(1)	82.4(2)	83.5(2)
S(1)–Zn–N(2)	82.6(1)	84.2(2)	83.6(2)
S(1)–Zn–N(1a)	97.3(1)	97.6(2)	96.5(2)
S(1)–Zn–N(2a)	97.4(1)	95.8(2)	96.4(2)
N(1)–Zn–N(2)	81.6(2)	79.7(2)	81.0(3)
N(1)–Zn–N(2a)	98.4(2)	100.3(2)	99.0(3)

$[\text{RhCl}_3(\text{[9]aneN}_2\text{S})] \cdot \text{H}_2\text{O}$

The compound $\text{RhCl}_3 \cdot \text{H}_2\text{O}$ reacts smoothly with [9]aneN₂S to form $[\text{RhCl}_3(\text{[9]aneN}_2\text{S})] \cdot \text{H}_2\text{O}$ in good yields. The presence of water of crystallization gives rise to rather sharp absorptions at 3510 and 3460 cm^{-1} in its IR spectrum. The NH vibrations are observed at 3210 and 3180 cm^{-1} . In the neutral half-sandwich complex $[\text{RhCl}_3(\text{[9]aneN}_2\text{S})]$, which is displayed in Fig. 4, rhodium(III) is octahedrally co-ordinated by [9]aneN₂S and three Cl atoms in a facial arrangement. The three five-membered chelate rings have $\lambda\lambda\lambda$ (or $\delta\delta\delta$) conformation.

The Rh–S bond of 2.246(1) Å (see Table 2) is considerably shorter than in the homoleptic rigorously octahedral $[\text{Rh}(\text{[9]aneS}_3)_2]^{3+}$,^{13,14} where bond lengths in the range 2.331(2)–2.348(2) Å have been observed. Probably a closer approach of the ligand is inhibited in the latter by a large number of non-bonding $\text{S} \cdots \text{S}$ contacts of 3.26 and 3.33 Å. In $[\text{RhCl}_3(\text{[9]aneN}_2\text{S})] \cdot \text{H}_2\text{O}$ only two non-bonding $\text{S} \cdots \text{Cl}$ contacts [3.251(1) and 3.276(1) Å] are present. The short Rh–S bond implies some Rh→S back donation. The Rh–S bond also exerts a slight structural *trans* influence on the Rh–Cl bond which is in the position *trans* to it. The Rh–Cl(1) bond is longer by 0.033 Å than the average Rh–Cl (*cis*) distance and this effect may well be caused by the participation of Cl(1) in two hydrogen bonds. The Rh–N bond lengths are 2.036(3) and 2.040(3) Å. For comparison Rh–N bond lengths in the range 2.08 to 2.28 Å have been found in $[\text{Rh}_2\text{H}_2(\mu\text{-H})_2\text{L}_2][\text{PF}_6]_2$ (L = 1,4,7-trimethyl-1,4,7-triazacyclonane, $\text{Me}_3\text{[9]aneN}_3$).¹⁵ In the solid state water of crystallization and complex molecules are interconnected by N–H \cdots Cl and O–H \cdots Cl hydrogen bonds.

[Ru(cym)([9]aneN₂S)][BPh₄]Cl₂·MeCN (cym = *p*-cymene)

Homoleptic ruthenium complexes of [9]aneN₃,^{16,17} Me₃[9]aneN₃^{18,19} and [9]aneS₃^{20–22} have been known for a long time. More recently half-sandwich complexes with these ligands, *e.g.* [Ru(cym)([9]aneN₃)²⁺ have been studied.^{23–25} Apart from structural interests some of the complexes show intriguing reactivities. The mixed-sandwich complex [Ru(cym)([9]aneN₂S)][BPh₄]Cl₂·MeCN was obtained by reaction of [RuCl₂(cym)]₂ with [9]aneN₂S in methanol. Ruthenium(II) was converted to ruthenium(III) during this reaction by aerial oxidation. The structure of [Ru(cym)([9]aneN₂S)]³⁺ is shown in Fig. 5; Table 4 contains selected bond lengths and angles. The Ru–S and Ru–N bond lengths are 2.324(2), 2.120(7) and 2.105(7) Å, respectively. The observed Ru^{III}–S bond length is slightly shorter than in [Ru([9]aneS₃)₂]²⁺.^{20–22} In the half-sandwich complexes [Ru([9]aneS₃)L₃]^{m+} (L = MeCN, Cl, PPh₃, PMe₂Ph, PEtPh₂ or CO) and others, significantly shorter Ru–S distances were found.^{24,25} Missing S···S non-bonding interactions as well as the nature of the coligands may account for this. As a consequence of the smaller radius of ruthenium(III) compared to ruthenium(II) the Ru–N bond lengths in [Ru(cym)([9]aneN₂S)]³⁺ and [Ru(cym)([9]aneN₃)²⁺ differ slightly. The macrocycle [9]aneN₂S displays a λλλ (or δδδ) configuration in the former. As in the starting compound *p*-cymene is η⁶ coordinated to the metal centre. The Ru–C bond lengths vary in the small range 2.196(7)–2.233(8) Å, with a mean distance of 2.214 Å. The complex cation displays approximately mirror

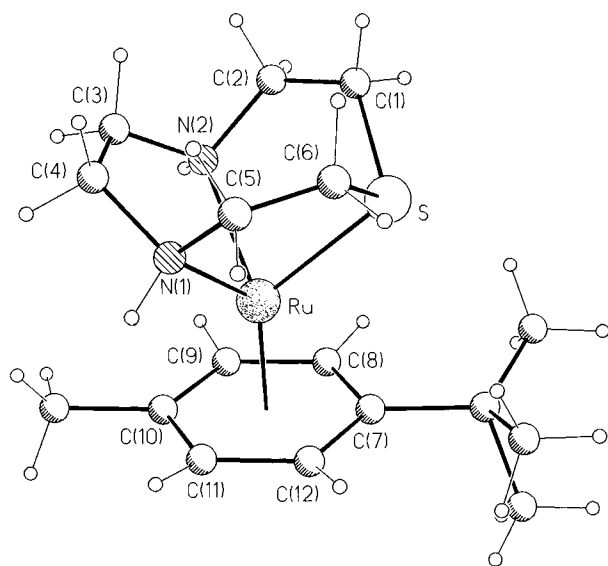


Fig. 5 Structure of [Ru(cym)([9]aneN₂S)][BPh₄]Cl₂·MeCN

symmetry. Three of the carbon atoms of the phenyl ring and the three macrocyclic donor atoms are eclipsed looking down the pseudo-three-fold axes of the complex.

[ReO₃([9]aneN₂S)][ReO₄]

It has been shown^{26–28} that [9]aneN₃ and [9]aneS₃ were able to form complexes with metals in very high oxidation states. We prepared the rhenium(VII) half-sandwich complex of [9]aneN₂S by reaction of dirhenium heptaoxide with the unco-ordinated macrocycle in tetrahydrofuran (thf) as described by Herrmann *et al.*²⁷ The compound was obtained in good yield, but attempts to grow single crystals failed. Its identity was proven by elemental analysis, IR and Raman spectroscopy, which gave the most valuable information. The two strong, well resolved bands 972 and 964 cm⁻¹ in the Raman spectrum have equal intensity and are assigned to the symmetric stretching vibration of the ReO₃⁺ and the ReO₄⁻ groups, respectively. The IR spectrum shows a broad and intense absorption at 910 cm⁻¹ with a shoulder at approximately 930 cm⁻¹. We assign these bands to the asymmetric stretching vibrations of the ReO₄⁻ and the ReO₃⁺ moieties. In [ReO₃([9]aneN₃)]⁺ and [ReO₃([9]aneS₃)]⁺ the relevant vibrations (IR spectra only) have been observed at 935 and 909, 921 and 912 cm⁻¹, respectively. Recrystallization of [ReO₃([9]aneN₂S)][ReO₄] from water yields the salts [H₂([9]aneN₂S)][ReO₄]₂ and [H([9]aneN₂S)][ReO₄], depending on the pH. Their crystal structures have been determined.²⁹

Table 4 Selected bond lengths (Å) and angles (°) for [Ru(cym)([9]aneN₂S)][BPh₄]Cl₂·MeCN and [Ti([9]aneN₂S)][ClO₄]

[Ru(cym)([9]aneN ₂ S)][BPh ₄]Cl ₂ ·MeCN			
Ru–N(1)	2.120(7)	Ru–C(7)	2.216(8)
Ru–N(2)	2.105(7)	Ru–C(10)	2.222(7)
Ru–C(9)	2.196(7)	Ru–C(8)	2.233(8)
Ru–C(11)	2.205(7)	Ru–S	2.324(2)
Ru–C(12)	2.213(8)		
N(2)–Ru–N(1)	79.4(3)	C(12)–Ru–S	104.3(2)
N(2)–Ru–S	83.2(2)	C(7)–Ru–S	90.1(2)
N(1)–Ru–S	82.8(2)	C(10)–Ru–S	170.3(2)
C(9)–Ru–S	138.5(3)	C(8)–Ru–S	104.7(2)
C(11)–Ru–S	137.2(2)		
[Ti([9]aneN ₂ S)][ClO ₄]			
Ti(1)–N(1)	2.68(2)	Ti(2)–N(3)	2.60(2)
Ti(1)–N(2)	2.66(2)	Ti(2)–N(4)	2.26(2)
Ti(1)–S(1)	2.920(8)	Ti(2)–S(2)	2.955(7)
N(2)–Ti(1)–N(1)	65.8(7)	N(3)–Ti(2)–S(2)	68.3(4)
N(2)–Ti(1)–S(1)	68.7(5)	N(4)–Ti(2)–S(2)	68.6(4)
N(1)–Ti(1)–S(1)	68.5(6)	N(3)–Ti(2)–N(4)	67.2(6)

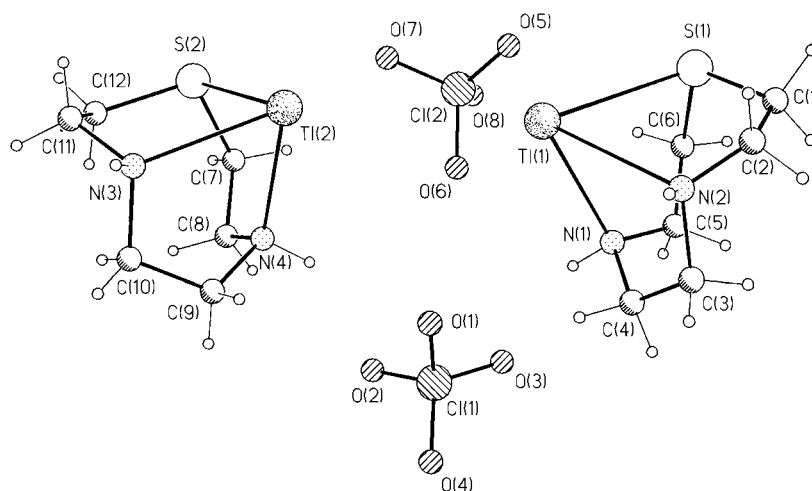


Fig. 6 Structure of [Ti([9]aneN₂S)][ClO₄]

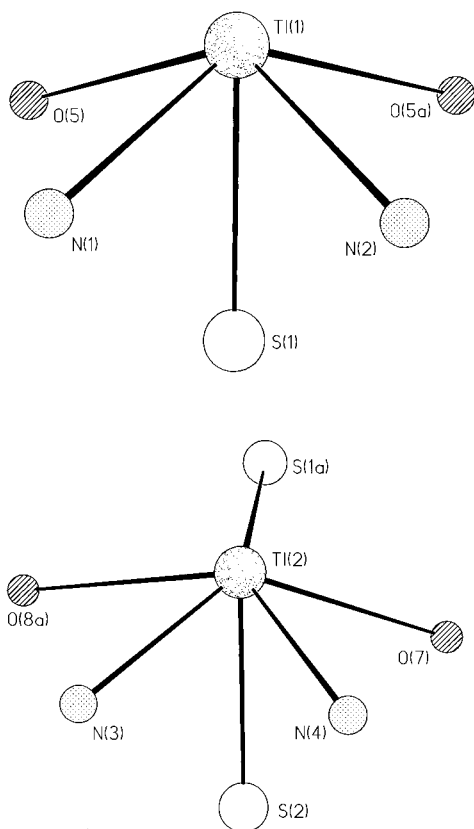


Fig. 7 Co-ordination around Tl(1) and Tl(2) in $[\text{Ti}(\text{[9]aneN}_2\text{S})][\text{ClO}_4]$

$[\text{Ti}(\text{[9]aneN}_2\text{S})][\text{ClO}_4]$

So far mainly transition-metal complexes of [9]aneN₂S have been described, whereas from the related nine-membered ligands a number of complexes with p block metal ions have been reported, e.g. $[\text{Pb}(\text{[9]aneN}_3)]\text{X}_2$ (X = ClO₄ or NO₃),³⁰ $[\text{Ti}(\text{Me}_3\text{[9]aneN}_3)]\text{PF}_6$ ³¹ and $[\text{Ti}(\text{[9]aneS}_3)]\text{PF}_6$.³² The structure of the latter is dominated by secondary Tl⋯S interactions. The complex $[\text{Ti}(\text{[9]aneN}_2\text{S})][\text{ClO}_4]$ was prepared from thallium(i) carbonate in methanol and recrystallized from water. In order to establish the connectivity and stereochemistry a structure determination was performed. The structure is composed of two slightly different ion pairs $[\text{Ti}(\text{[9]aneN}_2\text{S})]^+$ and ClO₄⁻ in the asymmetric unit. Their structure is shown in Fig. 6 and selected bond lengths and angles are given in Table 4.

The macrocycle [9]aneN₂S is bound facially to the metal centres, with Tl(1)–S(1) 2.920(8) and Tl(2)–S(2) 2.955(7) Å. The Tl–S bond lengths are less than the sum of the ionic radii of 3.34 Å and significantly less than the values of 3.092(3)–3.114(3) Å, found in $[\text{Ti}(\text{[9]aneS}_3)]\text{PF}_6$,³² thus suggesting substantial covalency. In addition to the primary co-ordination, there is a weak secondary interaction *via* exodentate co-ordination between S(1) and Tl(2), Tl(2)–S(1a) 3.761(3) Å. The Tl–N bond lengths at Tl(1) and Tl(2) differ slightly. The mean value exceeds the Tl–N bond lengths in $[\text{Ti}(\text{Me}_3\text{[9]aneN}_3)]\text{PF}_6$ by 0.04 to 0.08 Å. The X–Tl–Y angles (X, Y = N, S) are substantially narrower than those observed in the transition-metal complexes and reflect the large size of the Tl⁺ cation.

The atom Tl(1) is five-co-ordinate, if one includes intermolecular contacts at 3.179 and 3.347 Å to two oxygen atoms of the perchlorate ion, whereas Tl(2) is six-co-ordinate including contacts to oxygen atoms of the second perchlorate ion at 3.310 and 3.406 Å, and the exodentate interaction mentioned above. Atom Tl(1) is pseudo-octahedrally co-ordinated and Tl(2) is situated in a pseudo-pentagonal bipyramidal environment. At both metal centres the lone pair has a very distinct stereochemical influence. In both polyhedra all five, respectively six donor atoms are situated at the same side with respect to the

metal centres (see Fig. 7). The shortest Tl(1)⋯Tl(2) distance is 4.22 Å and [9]aneN₂S displays a λλλ (or δδδ) configuration in both cations.

Conclusion

The macrocycle [9]aneN₂S forms stable 1:1 and 1:2 complexes with a variety of main-group and transition metals in oxidation states I to VII. In the bis-complexes of 3d elements the metal–nitrogen and metal–sulfur bond lengths generally exceed the bond lengths in the corresponding homoleptic complexes of [9]aneN₃ and [9]aneS₃. Obviously the more symmetrical structure of these ligands, with equal distances between the donor atoms, allows a closer approach of these atoms towards the metal centre. For metal ions with larger radii, e.g. Tl^I, we observed a different situation. Here the metal–sulfur distance in the complexes of [9]aneN₂S is equal to or even smaller than that in the complexes of [9]aneS₃. The conformational strain exerted upon [9]aneN₂S upon co-ordination increases with decreasing radii of the metal ions. This is evident in the C–N–C angles and the X–C–C–X torsion angles. In this respect it is also interesting to compare the difference between the metal–nitrogen and the metal–sulfur bond lengths Δ(M–S, M–N) in the complexes studied. This value changes from 0.21 Å in $[\text{RhCl}_3(\text{[9]aneN}_2\text{S})]\cdot\text{H}_2\text{O}$ and $[\text{Ru}(\text{cym})(\text{[9]aneN}_2\text{S})][\text{BPh}_4]\text{Cl}_2\cdot\text{MeCN}$ to 0.39–0.40 Å in $[\text{Mn}(\text{[9]aneN}_2\text{S})_2][\text{ClO}_4]_2$ and $[\text{Zn}(\text{[9]aneN}_2\text{S})_2][\text{PF}_6]_2$.

We observed both λλλ and λδλ (the two rings coupled by the S atom have opposite chiralities) conformations of the three chelate rings formed. The conformational behaviour is independent of the metal-to-donor-atom bond lengths, Δ(M–S or of M–N). The conformation actually adopted seems to depend upon external forces.⁴

Experimental

CAUTION: Perchlorate salts are potentially explosive and should be handled with care.

All chemicals used for the preparative work were of standard reagent grade quality and were used without further purification.

Preparations

1-Thia-4,7-diazacyclononane ([9]aneN₂S). The macrocycle was prepared as described earlier² and stored as $[\text{9]aneN}_2\text{S}\cdot 2\text{HBr}$.

$[\text{VOCl}_2(\text{[9]aneN}_2\text{S})]\cdot\text{MeCN}$. A solution of [9]aneN₂S (146 mg, 1 mmol) in acetonitrile (20 cm³) was added to a boiling solution of VCl₃ (157 mg, 1 mmol) in acetonitrile (30 cm³). The reaction mixture was refluxed for 30 min under N₂, then filtered and cooled to –15 °C. Within a week light blue crystals of $[\text{VOCl}_2(\text{[9]aneN}_2\text{S})]\cdot\text{MeCN}$ (120 mg, 42%) separated, which loose solvent in air (Found: C, 24.7; H, 4.9; N, 9.9. Solvent-free C₆H₁₄Cl₂N₂O₂OSV requires C, 25.4; H, 4.95; N, 9.85%). $\tilde{\nu}_{\text{max}}/\text{cm}^{-1}$ (KBr disc): 3240s, 3200s (NH), 1020s, 985vs (VO), 946s, 791m, 354m, 275s (VCl). $\lambda_{\text{max}}/\text{nm}$ (ε/dm³ mol⁻¹ cm⁻¹) (EtOH): 362 (67), 505 (21) and 670 (63).

$[\text{Mn}(\text{[9]aneN}_2\text{S})_2][\text{ClO}_4]_2$. To a solution of [9]aneN₂S (293 mg, 2 mmol) in methanol (50 cm³) was added a solution of manganese perchlorate (300 mg, 2 mmol) in methanol (20 cm³). The combined solutions were stirred for a further 30 min under N₂. The compound crystallized upon standing at –20 °C as tiny air-sensitive needles (340 mg, 60%) (Found: C, 26.30; H, 5.25; N, 10.00. C₁₂H₂₈Cl₂MnN₄O₈S₂ requires C, 26.40; H, 5.15; N, 10.25%). $\tilde{\nu}_{\text{max}}/\text{cm}^{-1}$ (KBr disc): 3280s, 3130vs (br) (NH), 1090vs (vbr) (ClO), 800m, 635s, 625vs (ClO).

$[\text{Fe}(\text{[9]aneN}_2\text{S})_2][\text{ClO}_4]_2$. Under Ar a solution of [9]aneN₂S (150 mg, 1 mmol) in CHCl₃ was added to a solution of iron(II)

Table 5 Crystallographic data for the V^{IV}, Fe^{II}, Zn^{II}, Rb^{II}, Rb^{III}, Ru^{III} and Tl^I complexes

Formula	C ₆ H ₁₄ Cl ₂ N ₂ OSV	C ₁₂ H ₂₈ Cl ₂ FeN ₄ O ₈ S ₂	C ₁₂ H ₂₈ Cl ₄ N ₄ S ₂ Zn ₂	C ₆ H ₁₆ Cl ₃ N ₂ ORhS	C ₄₂ H ₃₁ BCl ₂ N ₃ RuS	C ₁₂ H ₂₈ Cl ₂ N ₄ O ₈ S ₂ Tl
M	325.1	547.3	647.8	373.5	812.7	900.1
Crystal system	Monoclinic	Monoclinic	Monoclinic	Triclinic	Triclinic	Monoclinic
Space group	P2 ₁ /c	P2 ₁ /c	P2 ₁ /c	P1	P1	P2 ₁ /c
a/Å	12.429(2)	8.079(2)	7.315(1)	7.304(1)	9.711(2)	13.520(3)
b/Å	7.270(1)	8.636(2)	16.899(3)	7.919(2)	11.006(2)	7.577(2)
c/Å	15.555(3)	14.960(4)	9.469(2)	10.475(2)	19.414(4)	23.353(5)
a°	—	—	—	86.55(3)	74.14(3)	—
β°	102.86(3)	90.01(2)	95.78(3)	89.44(3)	87.54(3)	91.73(3)
γ°	—	—	—	88.11(3)	89.72(3)	—
U/Å ³	1370.3	1043.8	1164.6	604.4	1994.1	2448
Z	4	2	2	2	2	4
D _c /g cm ⁻³	1.576	1.74	1.85	2.05	1.289	2.44
μ/mm ⁻¹	1.226	1.218	1.490	2.200	0.608	13.58
F(000)	688	568	656	372	806	1680
Crystal size/mm	0.1 × 0.12 × 0.18	0.1 × 0.2 × 0.13	0.1 × 0.15 × 0.18	0.1 × 0.15 × 0.15	0.05 × 0.06 × 0.17	0.2 × 0.11 × 0.12
2θ range/°	4–54	4–54	4–54	4–54	4–54	4–54
Data collected	3404	2291	2704	2453	9208	4656
Unique data	3012	1933	2512	2270	8688	4534
Data with F _o > 4σ(F _o)	2138	1139	1791	2139	4597	2231
Absorption correction	ψ scan	—	ψ scan	ψ scan	—	—
Parameters refined	213	169	151	191	213	220
g in weighting scheme	0.0002	0.0004	0.0004	0.0002	—	—
R	0.029	0.0613	0.059	0.023	0.075(R1)	0.099(R1)
R'	0.029	0.0686	0.073	0.029	0.226(wR2)	0.27(wR2)
Δρ(max.)/e Å ⁻³	0.84	0.65	0.63	0.66	1.07	3.86

$$R = \sum |F_o| - |F_c| / \sum |F_o|, R' = \sum [w(F_o - F_c)]^2 / \sum [w(F_o)]^2, R1 = \sum |F_o| - |F_c| / \sum |F_o|, wR2 = \sum [w(F_o^2 - F_c^2)]^2 / \sum [w(F_o^2)]^2$$

perchlorate (360 mg, 1 mmol) in ethanol (30 cm³). The resulting green precipitate of [Fe(9)aneN₂S]₂[(ClO₄)₂] (250 mg, 92%) was filtered off (Found: C, 27.25; H, 5.50; N, 9.70. C₁₂H₂₈Cl₂FeN₄O₈S₂ requires C, 26.35; H, 5.15; N, 10.25%). $\tilde{\nu}_{\max}/\text{cm}^{-1}$ (KBr disc): 3268s, 3104s (NH), 1090vs (br) (ClO), 625s (ClO). Single crystals of X-ray quality were obtained by slow diffusion of concentrated solutions of iron(II) perchlorate and the macrocycle.

[Zn(9)aneN₂S]₂[(PF₆)₂]. To a solution of zinc acetylacetonate (400 mg, 15 mmol) in methanol (30 cm³) was added a solution of [9]aneN₂S (450 mg, 3 mmol) in methanol (10 cm³). The clear solution was stirred for 1 h. Then NaPF₆ (1 g) was added to precipitate [Zn(9)aneN₂S]₂[(PF₆)₂] as a white solid (330 mg, 58%) (Found: C, 22.20; H, 4.15; N, 8.70. C₁₂H₂₈F₁₂N₄S₂P₂Zn requires C, 22.20; H, 4.30; N, 8.65%). $\tilde{\nu}_{\max}/\text{cm}^{-1}$ (KBr disc): 3310vs, 3110m (NH), 830vs (br) (PF), 550s (PF).

[Ru(cym)(9)aneN₂S][BPh₄]Cl₂·MeCN. A methanolic (10 cm³) solution of [9]aneN₂S (292 mg, 2 mmol) was added to a solution of [RuCl₂(cym)]₂ (306 mg, 0.5 mmol) in methanol (30 cm³). During this procedure the colour changed from red-orange to dark green. The reaction was stirred for a further 0.5 h and then a concentrated solution of potassium tetraphenylborate (680 mg, 2 mmol) in methanol was added. The light green precipitate which formed was filtered off and recrystallized from acetonitrile to yield (620 mg, 80%) colourless crystals (Found: C, 61.65; H, 5.90; N, 4.90. C₄₂H₅₁BCl₂N₃RuS requires C, 62.05; H, 6.30; N, 5.15%). $\tilde{\nu}_{\max}/\text{cm}^{-1}$ (KBr disc): 3241m (NH), 3053s (CH_{aryl}), 735s, 710s (CH_{aryl}).

[ReO₃(9)aneN₂S][ReO₄]. To a solution of dirhenium heptaoxide (242.2 mg, 0.5 mmol) in tetrahydrofuran (10 cm³) was added a solution of [9]aneN₂S (73.1 mg, 0.5 mmol) in the same amount of tetrahydrofuran to afford a white solid. This was filtered off and dried *in vacuo* (280 mg, 80%) (Found: C, 11.45; H, 2.30; N, 4.40. C₆H₁₂N₂O₇Re₂S requires C, 11.45; H, 2.25; N, 4.45%). $\tilde{\nu}_{\max}/\text{cm}^{-1}$ (KBr disc): 2980–2700m (CH), 1440m, 1420m (CH), 930vs (sh), 910vs (br) (ReO), 360m, 350m (ReO). Raman spectrum: 972vs [$\nu_{\text{sym}}(\text{ReO}_3)$], 964vs cm⁻¹ [$\nu_{\text{sym}}(\text{ReO}_4)$].

[RhCl₃(9)aneN₂S]·H₂O. Combined solutions of [9]aneN₂S (300 mg, 1.6 mmol) in ethanol (10 cm³) and rhodium trichloride hydrate (130 mg, 0.57 mmol) in ethanol (20 cm³) were refluxed for 0.5 h. Upon cooling a light brown solid precipitated from the clear solution. It was recrystallized from water to give yellow-orange crystals of [RhCl₃(9)aneN₂S]·H₂O (380 mg, 70%) (Found: C, 19.25; H, 4.30; N, 7.60. C₆H₁₆Cl₃N₂ORhS requires C, 19.30; H, 4.30; N, 7.50%). $\tilde{\nu}_{\max}/\text{cm}^{-1}$ (KBr disc): 3510m, 3460m (OH), 3210vs, 3180vs (NH), *ca.* 900, *ca.* 300 (RhCl).

[Tl(9)aneN₂S][ClO₄]. To a solution of thallium(I) carbonate (500 mg, 1 mmol) in water (50 cm³) was added a solution of [9]aneN₂S (750 mg, 5 mmol) in methanol (40 cm³) and solid NaClO₄ (10 mg, 8.2 mmol). The solution was concentrated slightly. White crystals of [Tl(9)aneN₂S][ClO₄] (250 mg, 55%) appeared within a few hours (Found: C, 16.0; H, 3.15; N, 6.05. C₆H₁₄ClN₂O₄STl requires C, 16.0; H, 3.15; N, 6.20%). $\tilde{\nu}_{\max}/\text{cm}^{-1}$ (KBr disc): 3310m (br), 3220s (NH), 1160vs (br), 625s (ClO).

Single-crystal structure determinations

Details of the crystal data, data collection and processing, and structure analysis are given in Table 5. The data for [VOCl₂(9)aneN₂S]·MeCN and [Ru(cym)(9)aneN₂S][BPh₄]Cl₂ were collected at 80 K using a Siemens R3m/V diffractometer, the data for the remaining compounds at ambient temperature by using an Enraf-Nonius CAD4 diffractometer, both equipped with graphite-monochromated Mo-K α radiation ($\lambda = 0.71073$ Å).

Lattice parameters were determined by least-squares fits to the setting parameters of 15–25 reflections. The structures were solved by Patterson methods (SHELXTL PLUS³³ program packages) and developed by iterative cycles of full-matrix least-squares anisotropic refinement for all non-hydrogen atoms and Fourier-difference syntheses. Except for the complexes of Ru^{III} and Tl, the quantity minimized was $\sum w(F_o - F_c)^2$ with the weighting scheme $w^{-1} = \sigma^2(F_o) + gF_o^2$ (for *g* values see Table 5). The structures of [Ru(cym)(9)aneN₂S][BPh₄]Cl₂ and [Tl(9)aneN₂S][ClO₄] were refined on *F*² using the program SHELXL.³⁴ In the structure of the former three of the four phenyl substituents of the [BPh₄]⁻ ion and the solvent molecule MeCN are disordered over two positions in the ratio 1 : 1. The disorder in the structure of [Fe(9)aneN₂S]₂[(ClO₄)₂] could be resolved by introducing split positions for two carbon atoms (see above) and for two oxygen atoms of the ClO₄⁻ ion. Hydrogen atoms were localized in difference syntheses for [VOCl₂(9)aneN₂S]·MeCN and [RhCl₃(9)aneN₂S]·H₂O and were placed for the remaining compounds in idealized positions with isotropic thermal parameters fixed at 0.08 Å².

Atomic coordinates, thermal parameters, and bond lengths and angles have been deposited at the Cambridge Crystallographic Data Centre (CCDC). See Instructions for Authors, *J. Chem. Soc., Dalton Trans.*, 1997, Issue 1. Any request to the CCDC for this material should quote the full literature citation and the reference number 186/340.

Physical measurements

Infrared spectra were measured on a Perkin-Elmer PE 683 instrument, Raman spectra on a Bruker IFS FT-Raman Module FRA 66 and EPR spectra on a Bruker ESP 300 X-band spectrometer. The UV/VIS spectra were recorded on solutions using a Shimadzu UV-3100 spectrometer. Microanalyses were performed by the Institute of Organic Chemistry of the Westfälische Wilhelms-University.

Acknowledgements

We thank the Fonds der Chemischen Industrie for financial support.

References

- 1 P. Chaudhuri and K. Wieghardt, *Prog. Inorg. Chem.*, 1987, **35**, 329; S. R. Cooper and S. C. Rawle, *Struct. Bonding (Berlin)*, 1990, **72**, 1; A. J. Blake and M. Schröder, *Adv. Inorg. Chem.*, 1990, **35**, 1.
- 2 P. Hoffmann, A. Steinhoff and R. Mattes, *Z. Naturforsch., Teil B*, 1987, **42**, 867; P. Hoffmann and R. Mattes, *Z. Naturforsch., Teil B*, 1988, **43**, 261; P. Hoffmann, F.-J. Hermes and R. Mattes, *Z. Naturforsch., Teil B*, 1988, **43**, 567; P. Hoffmann and R. Mattes, *Inorg. Chem.*, 1989, **28**, 2092; K. Wasielewski and R. Mattes, *Acta Crystallogr., Sect. C*, 1990, **46**, 1826; U. Heinzel and R. Mattes, *Polyhedron*, 1991, **10**, 19; U. Heinzel and R. Mattes, *Polyhedron*, 1992, **11**, 597; U. Heinzel and R. Mattes, *Inorg. Chim. Acta*, 1992, **194**, 157.
- 3 S. M. Hart, J. C. A. Boeyens, J. P. Michael and R. D. Hancock, *J. Chem. Soc., Dalton Trans.*, 1983, 1601; M. Nonoyama and T. Ishida, *Transition Met. Chem.*, 1984, **9**, 367; L. Fabbrizzi and D. M. Proserpio, *J. Chem. Soc., Dalton Trans.*, 1989, 229; J. C. A. Boeyens, S. M. Dobson and R. D. Hancock, *Inorg. Chem.*, 1985, **24**, 3073; R. D. Hancock, S. M. Dobson and J. C. A. Boeyens, *Inorg. Chim. Acta*, 1987, **133**, 221; D. M. Wambeke, W. Lippens, G. G. Hermans, A. M. Goeminne and G. P. van der Kelen, *Polyhedron*, 1992, **11**, 2989.
- 4 L. R. Gahan, T. W. Hambley, G. H. Searle, M. J. Bjerrum and E. Larsen, *Inorg. Chim. Acta*, 1988, **147**, 17; T. W. Hambley, L. R. Gahan and G. H. Searle, *Acta Crystallogr., Sect. C*, 1989, **45**, 864.
- 5 A. McAuley and S. Subramanian, *Inorg. Chem.*, 1990, **29**, 2830; A. J. Blake, R. D. Crofts, B. de Groot and M. Schröder, *J. Chem. Soc., Dalton Trans.*, 1993, 485; I. A. Kahwa, D. Miller, M. Mitchell and F. R. Fronczek, *Acta Crystallogr., Sect. C*, 1993, **49**, 320.
- 6 R. Bentfeld, N. Ehlers and R. Mattes, *Chem. Ber.*, 1995, **128**, 1199.
- 7 G. R. Willey, M. T. Lakin and N. W. Alcock, *J. Chem. Soc., Chem. Commun.*, 1991, 1414.

- 8 K. Wieghardt, U. Bossek, K. Volckmar, W. Swiridoff and J. Weiss, *Inorg. Chem.*, 1984, **23**, 1387.
- 9 L. R. Gahan, V. A. Grillo, T. W. Hambley, G. R. Hanson, C. J. Hawkins, E. M. Proudfoot, B. Moubaraki, K. S. Murray and D. Wang, *Inorg. Chem.*, 1996, **35**, 1039.
- 10 H.-J. Küppers, K. Wieghardt, Y.-H. Tsay, C. Krüger, B. Nuber and J. Weiss, *Angew. Chem.*, 1987, **99**, 583; *Angew. Chem., Int. Ed. Engl.*, 1987, **26**, 575.
- 11 R. Feldhaus, J. Köppe and R. Mattes, *Z. Naturforsch., Teil B*, 1996, **51**, 869.
- 12 H.-J. Küppers and K. Wieghardt, *Z. Anorg. Allg. Chem.*, 1989, **577**, 155.
- 13 S. C. Rawle, R. Yagbasan, K. Prout and S. R. Cooper, *J. Am. Chem. Soc.*, 1987, **109**, 6181.
- 14 A. J. Blake, R. O. Gould, A. J. Holder, T. I. Hyde and M. Schröder, *J. Chem. Soc., Dalton Trans.*, 1988, 1861.
- 15 D. Hanke, K. Wieghardt, B. Nuber, R.-S. Lu, R. K. McMullan, T. F. Koetzle and R. Bau, *Inorg. Chem.*, 1993, **32**, 4300.
- 16 K. Wieghardt, W. Herrmann, M. Köppen, I. Jibril and G. Huttner, *Z. Naturforsch., Teil B*, 1984, **39**, 1335.
- 17 P. Bernhard and A. M. Sargeson, *Inorg. Chem.*, 1988, **27**, 2582.
- 18 P. Neubold, K. Wieghardt, B. Nuber and J. Weiss, *Angew. Chem.*, 1988, **100**, 990; *Angew. Chem., Int. Ed. Engl.*, 1988, **27**, 933.
- 19 P. Neubold, K. Wieghardt, B. Nuber and J. Weiss, *Inorg. Chem.*, 1989, **28**, 459.
- 20 S. C. Rawle and S. R. Cooper, *J. Chem. Soc., Chem. Commun.*, 1987, 308.
- 21 S. C. Rawle, T. J. Sewell and S. R. Cooper, *Inorg. Chem.*, 1987, **26**, 3769.
- 22 M. N. Bell, A. J. Blake, A. J. Holder, T. I. Hyde and M. Schröder, *J. Chem. Soc., Dalton Trans.*, 1990, 3841.
- 23 S.-M. Yang, W.-C. Cheng, S.-M. Peng, K.-K. Cheung and C.-M. Che, *J. Chem. Soc., Dalton Trans.*, 1995, 2955 and refs. therein.
- 24 S. R. Cooper, *Acc. Chem. Res.*, 1988, **21**, 141.
- 25 A. J. Blake, R. M. Christie, Y. V. Roberts, M. J. Sullivan, M. Schröder and L. J. Yellowlees, *J. Chem. Soc., Chem. Commun.*, 1992, 848; A. F. Hill, N. W. Alcock, J. C. Cannadine and G. R. Clark, *J. Organomet. Chem.*, 1992, **426**, C40; N. W. Alcock, J. C. Cannadine, G. R. Clark and A. F. Hill, *J. Chem. Soc., Dalton Trans.*, 1993, 1131; J. C. Cannadine, A. Hector and A. F. Hill, *Organometallics*, 1992, **11**, 2323; C. Landgrafe and W. S. Sheldrick, *J. Chem. Soc., Dalton Trans.*, 1994, 1885.
- 26 H.-J. Küppers, B. Nuber, J. Weiss and S. R. Cooper, *J. Chem. Soc., Chem. Commun.*, 1990, 979.
- 27 W. A. Herrmann, P. W. Roesky, F. E. Kühn, W. Scherer and M. Kleine, *Angew. Chem.*, 1993, **105**, 1768; *Angew. Chem., Int. Ed. Engl.*, 1993, **32**, 1714.
- 28 K. Wieghardt, C. Pomp, B. Nuber and J. Weiss, *Inorg. Chem.*, 1986, **25**, 1659.
- 29 A. Henke, Ph.D. Dissertation, University of Münster, 1994.
- 30 K. Wieghardt, M. Kleine-Boymann, B. Nuber, J. Weiss, L. Zsolnai and G. Huttner, *Inorg. Chem.*, 1986, **25**, 1647.
- 31 K. Wieghardt, M. Kleine-Boymann, B. Nuber and J. Weiss, *Inorg. Chem.*, 1985, **25**, 1664.
- 32 A. J. Blake, J. A. Greig and M. Schröder, *J. Chem. Soc., Dalton Trans.*, 1991, 529.
- 33 G. M. Sheldrick, SHELXTL PLUS, Program package for structure solution and refinement, Version 4.2, Siemens Analytical Instruments Inc., Madison, WI, 1990.
- 34 G. M. Sheldrick, SHELXL 93, University of Göttingen, 1993.

Received 30th August 1996; Paper 6/05999F